

The Composition of Mica from the Salmi Batholith Granites as an Indicator of the Formation of Nb–Ta Mineralization

A. A. Konyshchev^{a, b, *}, Ya. O. Alferyeva^{c, **}, M. O. Anosova^{a, ***},
A. A. Rusak^{a, ****}, and Ya. I. Korepanov^{b, *****}

^aVernadsky Institute of Geochemistry and Analytical Chemistry, Russian Academy of Sciences, Moscow, 119991 Russia

^bKorzhinskii Institute of Experimental Mineralogy, Russian Academy of Sciences, Chernogolovka, Moscow oblast, 142432 Russia

^cDepartment of Geology, Moscow State University, Moscow, 119991 Russia

*e-mail: icelopa@gmail.com

**e-mail: YanaAlf@ya.ru

***e-mail: masha_anosova@mail.ru

****e-mail: aleks7975@yandex.ru

*****e-mail: yakoff@iem.ac.ru

Received October 25, 2018; revised December 3, 2018; accepted December 11, 2018

Abstract—Successive differentiates of acid rocks from the Salmi batholith are represented by the following series: biotite–amphibole rapakivi granite, biotite granite, and highly differentiated granites (Li-siderophyllite and Li–F zinnwaldite varieties). There is a gradual increase in the content of Ta and Nb and a decrease in the Nb/Ta ratio in this rock series. A regular change in the Ta and Nb partitioning coefficients between mica and the bulk rock composition is observed as well. Comparison of Li-siderophyllite granite and Li–F granite shows that the latter has a sharp decrease in the partitioning coefficients $K_{pTa, Nb}$. This is due to a decrease in the content of these metals in zinnwaldite from Li–F granite and associates with the appearance of columbite in these rocks. The study of rock samples from the Salmi batholith suggests that such change of the Ta and Nb content in the mica from deeply differentiated granite and the corresponding decrease in the K_p value of these metals may be diagnostic evidence of the presence of columbite mineralization in the rock.

Keywords: mica, A-type granite, rapakivi granite, rare-metal granite, Li–F granite

DOI: 10.3103/S0145875219040045

INTRODUCTION

The Salmi batholith relates to the anorthosite–rapakivi granite rock complexes (ARGC), whose acid rocks thought to be as intraplate granites of type A (Larin, 2011). The acid rocks of the Salmi batholith form a series of successive melt differentiates from biotite–hornblende rapakivi granite to rare-metal Li–F granite. The endogenic Ta and Nb deposits associate with such-like deeply differentiated granite (Zaraisky et al., 2008).

The compositional variations in acid magma differentiates and minerals and regularities in the Ta and Nb distribution between the different phases allow us to study the evolution of magmatic systems of the ARGC and the processes of accumulation of rare metals based on the example of the Salmi batholith.

GEOLOGICAL REVIEW

The Salmi batholith is located in southern Karelia, on the eastern shore of Lake Ladoga. The batholith is

composed of various rocks that formed 1547–1530 m.y. ago (Amelin et al., 1997), from gabbro and anorthosite to Li–F granite. The protolith of granitic rocks of this batholith includes the lower crustal rocks of the Svecofennian age and Karelian Craton (Newmark et al., 1994).

In the area of Pitkäranta, the batholith shallow dipping beneath the metasedimentary carbonate-bearing Paleoproterozoic cover that contain numerous skarn, greisen, and pegmatite deposits and ore occurrences. Many insignificant thickness bodies of topaz-bearing Li-siderophyllite (Li-*Sdph*) and Li–F zinnwaldite (Li-F) granites are outcropped in this part of the batholith, while most of them is hidden at depth. The massive Li-*Sdph* granite is exposed in the quarry for building materials in the Lupikko gneiss-granite dome; based on drilling data (Pavlov, 1991), Li–F granite occurs beneath the Uksinskii dome. The schematic map of the sampling is shown in Fig. 1.

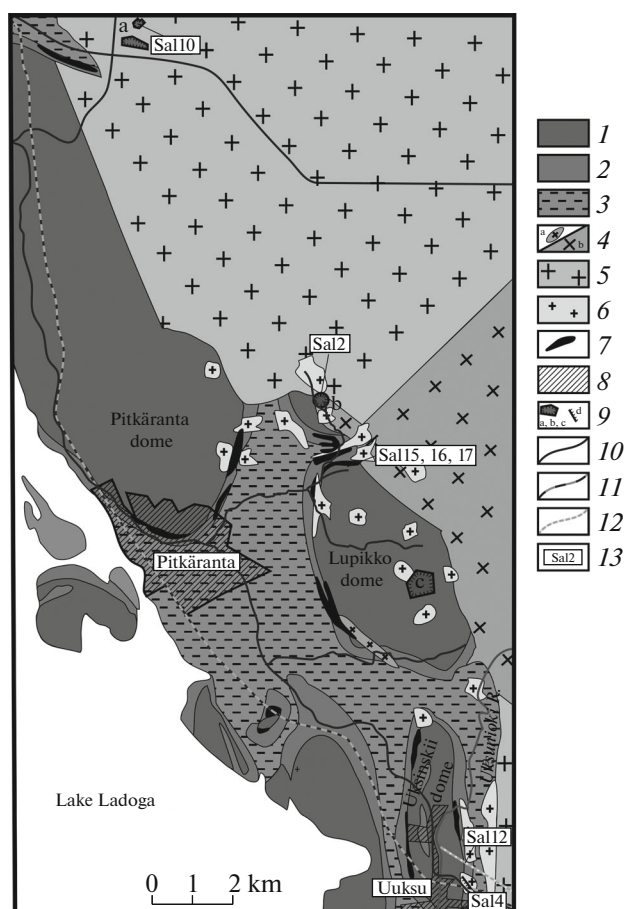


Fig. 1. A schematic map of the Pitkäranta area (northwestern part of the Salmi batholith, southern Karelia) with points of sampling, (modified after Ivashchenko and Golubev, 2015; Larin, 2011). (1) Gneiss-granite of the domes (AR₂–PR₁); (2) Sortavala Group: amphibolites, amphiboles, graphite and graphite-bearing schists, dolomite and apodolomite calcite marble and skarn after it; (3) Ladoga Group: biotite–quartz, quartz–feldspar–biotite, sometimes amphibole- and graphite-bearing schist with interbeds of hornfels and skarnoids; (4) biotite–hornblende granite (phase I): (a) rhyolite-porphyry, (b) coarse-granular varieties; (5) coarse- and fine-granular biotite granite (phase II); (6) areas with dykes of highly differentiated topaz-bearing Li–F and Li–*Sdph* granite; (7) skarn, greisenized skarn, and low-temperature metasomatic rocks after them, with the Fe–Cu–Zn–Sn and rare-metal mineralization; (8) residential development (showing Pitkäranta and Uuksu); (9) mines: (a) Repomyaki, (b) Mustavaara (not in a scale), (c) Mosavtodor crushed stone quarry, (d) outcrops on the sides of motor roads); (10) motor roads; (11) railway; (12) power line clearing; (13) sample no. and place.

MATERIALS AND METHODS

The major- and trace-element compositions of rocks were analyzed by the XRF and ICP-MS methods; their mineral composition was studied using X-ray spectral microanalysis. Due to the presence of mechanical impurities in micas, their microcomponent composition was studied using point analysis methods to avoid distortion of the result, that is, LA-ICP-MS and SIMS for Li and OH (Vasilyev and Borodulin, 2010).

The petrochemical composition of rocks was analyzed by the XRF method at the Institute of Geology of Ore Deposits, Petrography, Mineralogy, and Geochemistry of the Russian Academy of Sciences on an Axios mAX sequential vacuum spectrometer. Analysis was performed by the 439-RS NSAM VIMS method-

ology, which provides results of accuracy category III, according to GOST RF 41-08-205-04. The total iron in the samples was analyzed as Fe₂O₃.

The content of trace elements was analyzed by the ICP-MS method at the Institute of Mineralogy, Geochemistry, and Crystallochemistry of Rare Elements on an Elan 6100 DRC mass spectrometer. Two types of sample preparation were applied for transition of samples into a solution. The first type included the decomposition of samples and their transition into a solution; the second type of sample preparation was performed by fusing samples with lithium metaborate and further dissolution of the obtained bead. The second type of sample preparation contributes to a more correct conversion of REEs into the analyzed solution from granitoids, as was demonstrated based on the

example of methodological work with different types of sample preparation (Yasnygina and Rasskazov, 2008). The instrument drift and matrix effects were taken into account using an internal standard, as well as by periodic measurement of a control sample (GSR-2 and BCR-2). Each sample was analyzed from solutions prepared by the different methods. The discrepancy between parallel measurements did not exceed 10 rel %.

The study of the major-component composition of mica was carried out at the Laboratory of Local Methods of Matter Study of the Chair of Petrology at the Department of Geology of Moscow State University on a JEOL JXA 8230 electron microprobe equipped with five wavelength spectrometers. The analysis was performed at an accelerating voltage of 15 kV, a probe current of 30 nA, and a focused electron beam. Synthetic and natural silicates, pure metals, and metal oxides were used as standards.

The minor and trace-element composition of micas was studied by the LA-ICP-MS method, mostly at the Institute of Geology of Ore Deposits, Petrography, Mineralogy, and Geochemistry of the Russian Academy of Sciences; some analyses of the Nb content were performed at the Institute of Geochemistry and Analytical Chemistry of the Russian Academy of Sciences. Mineral grains mounted in epoxy were used for the study.

Analyses at the Institute of Geology of Ore Deposits, Petrography, Mineralogy, and Geochemistry of the Russian Academy of Sciences were carried out on an X-Series II mass spectrometer with ionization in inductively coupled plasma, in combination with a NWR-213 system of sample preparation. Samples of the NIST SRM 610 and 612 silicate glasses were used as standards. The diameter of the ablation crater was 60 μm ; the time of analysis was 30 s. The error of the analysis was 1–10 rel %.

Analyses at the Institute of Geochemistry and Analytical Chemistry of the Russian Academy of Sciences were performed on an Element XR mass spectrometer with ionization in inductively coupled plasma and with an UP-213 laser system of sample preparation. The NIST 610 and ML3B silicate glasses were used as standards. The diameter of the ablation crater was 30 μm ; the time of analysis was 30 s. The error of analysis for different elements was 1–10 rel %.

The contents of Li and OH in micas were analyzed on a Cameca ims-4f secondary-ion mass spectrometer at the Yaroslavl Branch Physical–Technological Institute of the Russian Academy of Sciences. Olivine was used as an anhydrous standard.

To verify the data on the Li content in mica, the content of Li was calculated from the empirical regularity that was obtained from the study of natural mica

of the siderophyllite–zinnwaldite type from A-type granites, according to (Tischendorf, 1997):

$$\text{Li wt \%} = \left(0.177(\text{F wt \%})^{1.642}\right)/2.1528. \quad (1)$$

The data on the composition of mica were averaged; the number of analyses is given in Tables 3 and 4.

PETROGRAPHIC DESCRIPTION OF ROCKS

The samples of granite of the different stages of differentiation were studied for the Salmi batholith.

Ovoid biotite–hornblende granite (Sample Sal2) is a rock composed of giant-granular ovoids of potassium feldspar (*Kfs*), often with an oligoclase rim, in the fine–medium-granular groundmass of the quartz–oligoclase–*Kfs*–biotite–hornblende composition. *Kfs* are irregularly distributed in the rock, from bulk predominance to their almost complete disappearance. The sizes of *Kfs* phenocrysts range from 10 to 50 mm. On the average, the size of matrix minerals is 1 mm; the size of quartz crystals sometimes reaches 5–8 mm; mica crystals are up to 4–5 mm. The content of rock-forming minerals in the groundmass is: 40–45% quartz (*Q*), 25–30% orthoclase (*Or*), and 20–25% plagioclase (*Pl*).

Biotite granite is represented by medium-granular *Q*–*Kfs*–oligoclase–biotite rock (Sample Sal10). It contains up to 5% biotite and almost equal proportions of *Q*, *Pl*, and *Kfs* (%): 30–35 *Q*, 25–30 *Pl*, and 25–30 *Or*. Crystals of feldspar have a size of 5–10 mm; dark pea-shaped *Q*, 1–3 mm; and biotite, up to 4–5 mm. There are variations in grain sizes over different outcrops up to fine-granular granite (the grain size is up to 1 mm, with rare inclusions of *Kfs* up to 5 mm and pea-shaped *Q* up to 1–3 mm) with the same quantitative proportions of the minerals.

Li-siderophyllite (Li-*Sdph*) granite (Samples Sal15, Sal16, and Sal17) form dikes of small thickness (1–2 m) that are injected in the Lupikko gneiss-granite dome. In general, the structure is massive. At times the rocks are slightly banded, which is related to the irregular distribution of mica (from 2 to 10%). Euhedral mica laths with a size up to 1 cm occur in the fine-granular (up to 1 mm) groundmass composed of *Q*, K–Na feldspar, and albite (*Ab*). The contents of rock-forming minerals in the samples are the following (%): 45 *Q*, 30 *Or*, 15–20 *Ab* (Sample Sal15); 30–35 *Q*, 15–20 *Or*, 40 *Ab* (Sample Sal16); 40 *Q*, 15–20 *Or*, 35 *Ab* (Sample Sal17). The rocks are poorly albitized; topaz is rare.

Zinnwaldite Li–F granite (Samples Sal4 and Sal12) forms dikes of the low thickness (from a few cm to 80 cm) injecting the Uksinskii gneiss-granite dome. This rock is composed of *Q*, *Kfs*, *Ab*, zinnwaldite, and topaz. The dikes of Li–F granite are essentially heterogeneous according to their mineral composition, as

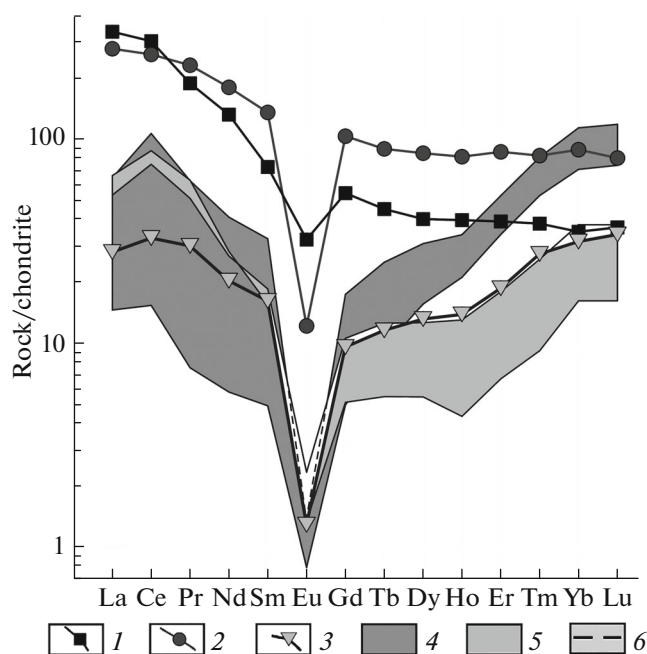


Fig. 2. The chondrite-normalized (Anders and Grevesse, 1989) REE spectra of the studied granites (Salmi batholith). (1) biotite–amphibole granite; (2) biotite granite; (3) massive Li–F granite, Sample 403-13 (Larin, 2011); (4) Li–*Sdph* granite; (5) Li–F granite; (6) upper edge of the field of Li–*Sdph* granite.

well as their textural and structural patterns. They have a banded or taxitic structure. The banding results from variations in the relative proportions of *Ab*, *Kfs*, *Q*, and mica, as well as from alternation of fine-granular, equigranular areas with a massive structure (aplite) and pegmatoid areas. The pegmatoid areas in dikes form bands or lenses with a thickness up to 10 cm. The borders between the aplitic and pegmatoid areas are sharp, clear, and oriented along the dike contacts.

The content of mica is less than 1% in the most leucocratic bands and 25–30% in melanocratic ones. Micas fill the interstitials between *Ab*, *Q*, *Kfs*, and topaz; the relative content of *Qz/Ab/Kfs* ranges within (12–50)/(30–70)/(12–40)% from the total content of these minerals. The grain size of minerals in the pegmatoid areas is 15–20 mm (*Q*) and up to 40 mm (*Kfs*). The contents of rock-forming minerals are (%): 25–30 *Q*, 10 *Or*, 45–50 *Ab*, 10 *Toz* (Sample Sal4); 30–35 *Q*, 5–10 *Or*, 50 *Ab*, and 5 *Toz* (Sample Sal12). The content of topaz in the rock is high but not stable (5–15%).

Li–F granite contains acicular crystals of columbite, which are mostly accumulated as inclusions in topaz. Fluorite is registered as inclusions in topaz, as well as in the interstitials between the minerals; its content in the rock is less than 1%.

According to the drilling data (Pavlov, 1991), an intrusive body of layered Li–F granite, occurs beneath the Uksinskii dome. The composition of Sample 403-13 from a drillhole (a depth of more than 300 m) was reported by Larin (2011); it is almost identical to Sam-

ples Sal4 and Sal12 according to the chondrite-normalized spectrum of rare elements. In this regard, we assume that these dikes are genetically related to the Li–F granite located beneath the Uksinskii dome. The chondrite-normalized REE spectra for the studied rocks (Anders and Grevesse, 1989) are shown in Fig. 2.

RESULTS AND DISCUSSION

A gradual decrease in the contents of iron and magnesium, an increase in the amount of sodium, and a decrease in the potassium content were registered from ovoid biotite–hornblende granite and biotite granite to topaz-bearing Li–*Sdph* and Li–F granites (Table 1). The degree of differentiation of the studied rocks, as characterized by the K/Rb ratio, varies from 230 in biotite–hornblende ovoid granite to 20–22 in Li–F granite (Table 2).

With an increasing degree of granite differentiation, the rocks become generally depleted in REEs (Fig. 2); a slight increase in the concentrations was detected for Er, Tm, Yb, and Lu in Li–*Sdph* granite. Li–F granite is remarkably depleted in all REEs in relation to other rocks. Their spectra are almost identical according to the shape and REE concentration to the REE spectra of Phanerozoic Li–F granite and ongonite (Kovalenko et al., 1983). An increase in the HREE/LREE ratio is observed in the considered series of differentiates.

Table 1. The chemical composition of rocks from the Salmi batholith

Composition	<i>Bt–Amp</i> granite	<i>Bt</i> granite	Li- <i>Sdph</i> granite			Li–F granite	
	Sal2	Sal10	Sal15	Sal16	Sal17	Sal4	Sal12
SiO ₂	71.17	73.79	77.42	73.55	74.95	72.91	74.38
TiO ₂	0.30	0.14	0.06	0.07	0.03	0.02	0.01
Al ₂ O ₃	14.24	12.88	11.89	14.32	13.87	17.07	15.49
Fe ₂ O ₃	3.10	2.30	1.82	1.64	1.33	0.72	0.96
MnO	0.04	0.02	0.02	0.01	0.01	0.04	0.03
MgO	0.21	0.07	0.03	0.06	0.02	0.05	0.04
CaO	0.66	0.74	0.08	0.22	0.26	0.21	0.10
Na ₂ O	2.83	3.38	2.34	5.01	4.63	6.32	6.64
K ₂ O	6.15	4.89	5.11	2.96	3.48	1.93	1.04
P ₂ O ₅	0.03	<0.02	<0.02	<0.02	<0.02	<0.02	<0.02
L.O.I.	0.91	0.92	0.85	0.78	1.22	0.66	1.06
F	–	0.49	0.32	<0.1	0.22	1.05	0.75
S	<0.02	<0.02	<0.02	<0.02	<0.02	<0.02	<0.02
Total	98.73	98.70	99.09	97.84	98.80	100.32	99.44
Total + L.O.I.	99.64	99.62	99.94	98.62	100.02	100.98	100.50

(–) Not analyzed.

All studied granite samples are characterized by a negative Eu anomaly, which becomes deeper with increasing degree of crystallization differentiation. The lowest Eu concentration is typical of Li-*Sdph* and Li–F granites. These rocks show an M type tetrad effect (Masuda et al., 1987), which is the clearest for the third and fourth tetrads. With account for the analytical error of the ICP-MS method, the tetrad effect is considered significant, if $TE > 1.1$. The most correct estimates are given by the joint use of the first, third, and fourth tetrads ($TE_{1,3,4}$) in the calculations (Irber, 1999; Yasnygina and Rasskazov). The total effect for the first, third, and fourth tetrads ($TE_{1,3,4}$), as estimated from the data of (Irber, 1999), is reported in Table 2.

Li–F granite is characterized by a low Y/Ho ratio (15.7–14.3), while in all other studied rocks, this value is 20.7–26.6 (Table 2); the chondritic value is 28 (Anders and Grevesse, 1989). Decrease in the Y/Ho ratio in residual melts may result from removal of Y with the brine fluoride melts formed at the late stages of consolidation of granite intrusions (Gramenitskiy and Shchekina, 2005; Peretyazhko and Savina, 2010; Veksler, 2005), as well as from crystallization of yttrium-rich minerals, such as fluorite, which, according to the data of X-ray spectral microanalysis, incorporates up to 0.6–0.65 wt % Y.

A regular increase in the Ta and Nb contents is observed in this rock series with an increasing degree of crystallization differentiation (Table 2). This is explained by redistribution of these metals into the residual silicate melt. The Nb/Ta values in the series of successive differentiates decrease from 12 to 1.6; Zr/Hf decreases from 38 to 5.1. According to the Nb/Ta and Zr/Hf values these rocks are beyond the boundaries of promising Ta-ore objects: Nb/Ta = 1 and Zr/Hf = 5 (Zaraisky et al., 2008), whereas the most differentiated varieties of Li–F granite are very close to them (Fig. 3).

Ta and Nb are incorporated in micas in the form of isomorphic impurities. In all studied rock types, their content in mica is higher than the bulk content in the rock. This feature is retained even when ore Ta–Nb minerals, in particular, columbite, are formed in the rock. In this regard, it is of interest to compare the contents of Ta and Nb in mica and in the bulk composition of granite with and without Ta–Nb mineralization. The ratio of the Ta and Nb concentration in mica to the concentration of these elements in the described granite varieties is shown in Fig. 4. Since the rocks contain a small (up to 10%) amount of mica, the data we obtained are close to the values of the Ta and Nb partitioning coefficients between mica and the silicate melt.

Table 2. The trace-element composition of rocks from the Salmi batholith, ppm

Composition	<i>Bt–Amp</i> granite	<i>Bt</i> granite	Li– <i>Sdph</i> granite			Li–F granite	
	Sal2	Sal10	Sal15	Sal16	Sal17	Sal4	Sal12
Li	51	101	182	76	91	453	370
Be	3.2	17.14	5.27	8.04	8.43	11.08	11.25
B	10.63	8.48	4.5	8.8	3.9	9.72	4.6
V	5.94	1.39	1.87	4.47	1.11	0.79	0.76
Co	1.4	0.82	0.45	0.48	0.84	0.65	0.52
Cu	2.6	3.09	3.07	3.56	4.41	5.43	2.73
Zn	86.86	92.37	24	11.4	17.8	59.36	13.7
Ga	25.73	38.28	26.07	29.07	26.87	70.21	33.77
Ge	1.92	1.89	3.62	3.21	2.98	<DL	2.8
As	1.58	<DL	1.94	1.33	1.82	<DL	0.90
Rb	222	335	586	347	504	639	395
Cs	3.32	3.66	2.69	1.28	1.28	6.91	2.64
Sr	127	69	15	17	19	64	60
Ba	1278	164	0.4	10	3	116	5
Zr	444	338	88	90	83	57	41
Hf	11.8	14.1	9.5	10.6	11.2	10	7.9
Nb	33.6	88.2	74.7	62.1	106.4	101.3	114.4
Ta	2.85	6.63	22.54	16.14	34.44	38.62	70.04
Mo	0.53	1.27	1.59	1.32	2.64	<DL	1.66
Sn	6.14	14.35	11.87	5.58	4.61	12.06	4.5
W	1.3	3.12	4.99	2.51	4.01	4.55	6.1
Ag	1.53	0.87	0.45	0.4	0.41	<DL	0.24
Tl	1.32	1.83	1.76	0.963	1.32	2.23	0.786
Pb	22.1	38.1	23.6	20.5	28.8	19.5	12.2
Bi	0.03	0.02	0.01	0.02	0.06	0.01	0.03
Th	22.5	35.9	44.9	26.3	39.8	28.4	26.4
U	2.85	10.58	8.97	8.96	6.85	5.54	3.71
Y	59.13	119.3	29.53	31.53	39.03	11.32	3.48
La	78.7	64.9	3.41	5.02	15.13	12.47	15.53
Ce	181.6	156.4	9.21	12.3	64.1	45.29	52.8
Pr	16.68	20.49	0.673	0.99	5.56	4.56	5.6
Nd	59.61	80.91	2.6	3.05	18.69	12.08	12.69
Sm	10.72	19.83	0.72	0.7	4.77	2.71	2.23
Eu	1.8	0.68	0.04	0.14	0.07	0.13	0.08
Gd	10.65	20.3	0.98	0.99	3.41	2.07	1.01
Tb	1.65	3.25	0.35	0.33	0.9	0.45	0.2
Dy	9.83	20.63	3.76	3.98	7.45	3.05	1.32
Ho	2.22	4.55	1.17	1.17	1.89	0.72	0.24
Er	6.26	13.73	5.41	5.99	8.39	2.84	1.06
Tm	0.93	2	1.28	1.32	1.97	0.62	0.22
Yb	5.7	14.41	11.52	11.62	18.42	6.17	2.61
Lu	0.89	1.96	1.83	1.83	2.87	0.92	0.39
K/Rb	230.5	121.2	72.4	70.8	57.3	25	21.8
Zr/Hf	37.6	23.9	9.3	8.5	7.4	5.6	5.1
Nb/Ta	11.8	13.3	3.3	3.8	3.1	2.6	1.6
Y/Ho	26.6	26.2	25.3	27	20.7	15.7	14.3
$TE_{1,3,4}^*$	1	1.02	1.19	1.2	1.29	1.29	1.32

* The value of the tetrad effect in the first, third, and fourth tetrahedra of REEs; <DL, below the detection limit.

Table 3. The minor and trace-element composition of the micas, ppm

Composition	<i>Bt–Amp</i> granite		<i>Bt</i> granite	<i>Li–Sdph</i> granite			<i>Li–F</i> granite	
	Sal2 Ov	Sal2 Osn	Sal10	Sal15	Sal16	Sal17	Sal4	Sal12
Li*	694	–	1367	5523	4287	3662	17380	12973
Li**	730	926	2145	4295	4197	3948	16230	13627
Li	426	518	3059	5252	5354	5064	13357	14210
Ti	17419	16908	21407	8321	7799	5963	1398	1437
Zn	740	742	2710	1461	796	1924	773	1021
Ga	41	53	253	253	226	244	108	154
Ge	<DL	<DL	11	10	10	13	3	6
Rb	544	573	2639	4599	4602	5698	7462	7618
Y	3	18	<DL	32	<DL	17	1	<DL
Nb	71	441	741	822	304	748	109	164
Sn	<DL	35	200	358	287	129	103	219
Ba	946	481	64	7	11	4	11	26
Ta	4	15	65	147	141	443	117	112
W	<DL	1	2	20	18	10	36	24
Tl	<DL	<DL	20	25	24	33	22	31
Number of analyses**	3	2	3	3	3	3	4	3
Number of analyses	2	2	6	7	4	6	20	5

Analyses were performed using the LA-ICP-MS method; * calculated data, after (Tischendorf, 1997); ** SIMS data. Ov, mica from the ovoid rim; Osn, mica from the groundmass.

The value of a partitioning coefficient $K_{pNb} = Nb_{mica}/Nb_{rock}$ gradually decreases in the differentiation series. The highest value of K_{pNb} (13) is typical of biotite from the groundmass of ovoid granite. With the transition to biotite granite, $K_{pNb} = 8$. On average, K_{pNb} for the biotite–rock pair is close to 10. This result is in a good agreement with the data of (Acosta-Vigil et al., 2010; Nash and Crecraft, 1985), according to which the values of the coefficient of Nb partitioning between the acid melt and biotite (K_{pNb}) are 8.7–9.1.

The most significant decrease in K_{pNb} occurs upon transition from *Li–Sdph* granite to zinnwaldite *Li–F* granite. The value of K_{pNb} decreases almost to 1; the concentrations of Nb in mica and in the bulk composition of rocks become almost equal. K_p for Ta shows increase from 5 to 10 at the earliest stages of differentiation and decrease in the latest rock varieties to ~2.

The values of K_p we obtained provide evidence for significant scattering of Nb and Ta in the crystalline material of rocks in the course of the mica formation. The probability of accumulation of these metals in successive differentiates of granite melt is limited by the content of micas and other dark-colored minerals formed at the different stages of intrusion consolidation. The high content of biotite in the early products of crystallization may prevent accumulation of these minerals in residual portions of deeply differentiated granite melt (Alferyeva et al., 2018a).

Variations in the values of K_{pNb} and K_{pTa} between mica and rock may be caused by several factors: (1) the low values of K_p for metals at the final stages of differentiation may be explained by the properties of micas (*Li–siderophyllite* and *zinnwaldite*); (2) a decrease in K_p for metals may result from variations in the $P–T$

Table 4. The composition of micas from the Salmi batholith, wt %

Composition	<i>Bt–Amp</i> granite		<i>Bt</i> granite	Li– <i>Sdph</i> granite			Li–F granite	
	Sal2 Ov	Sal2 Osn	Sal10	Sal15	Sal16	Sal17	Sal4	Sal12
TiO ₂	3.66	0.19	1.12	0.91	0.7	0.67	0.15	0.18
V ₂ O ₃	0.02	0.02	0.01	0.01	0.01	0.01	<DL	0.01
MnO	0.4	0.37	0.31	0.35	0.3	0.37	0.90	0.61
FeO	32.96	42	37.29	26.01	26.15	27.61	13.54	16.56
MgO	2.56	3.57	0.28	0.03	0.04	0.05	0.07	0.2
Al ₂ O ₃	12.31	15.4	15.78	18.79	19.44	19.26	19.68	20.6
SiO ₂	33.96	24.82	31.29	36.08	36.45	35.36	43.96	41.47
Cr ₂ O ₃	0.01	<DL	0.03	0.06	0.02	<DL	0.01	0.03
NiO	<DL	<DL	<DL	0.01	<DL	0.01	<DL	<DL
ZnO	0.17	0.16	0.24	0.13	0.08	0.16	0.13	0.1
CaO	0.01	0.02	<DL	0.02	0.01	0.01	<DL	0.01
BaO	0.14	<DL	0.01	0.01	0.01	0.01	<DL	<DL
Na ₂ O	0.07	0.01	0.11	0.19	0.13	0.14	0.19	0.2
K ₂ O	8.98	0.16	6.98	9.62	9.78	9.57	10.24	10.05
OH (SIMS)	3.59	2.42	3.23	3.37	3.57	3.50	1.81	2.83
Cl	0.56	0.02	0.39	0.12	0.14	0.2	0.01	0.02
F	0.90	<DL	1.36	3.19	2.73	2.48	6.41	5.37
Total	100.29	89.16	98.44	98.90	99.57	99.39	97.10	98.23
F/Cl	1.61	0	3.04	28.01	20.41	12.44	1873.8	422.89
Number of analyses	3	2	5	5	5	5	5	5

<DL, below the detection limit; Ov, mica from the ovoid rim; Osn, mica from the groundmass of *Bt–Amp* rapakivi granite.

parameters of crystallization; and (3) a significant decrease in K_p for metals between mica and rock with transition to Li–F granite may be explained by the beginning of columbite crystallization.

Successive differentiates of granite melt up to Li–F granite show gradual increase in the concentrations of Ta and Nb (Table 2). This is noted for all mica from investigated granites, excepting Li–F granite (Table 3). The concentrations of these metals decrease in zinnwaldite from columbite-bearing Li–F granite. The data from the study of rock samples from the Salmi batholith allow us to assume that sharp change in the concentration of Ta and Nb in micas from deeply differentiated granite and the corresponding decrease in K_p of these metals may indicate the presence of columbite mineralization in the rock.

It is necessary to mention that the correlation between columbite and the low concentration of Ta and Nb in mica was registered for the late crystalliza-

tion differentiation of melt only. Figure 4 shows that $K_{pNb,Ta}$ between biotite contained in ovoids in rapakivi granite and rock has values close to 1–2. According to the data of Shebanov et al. (1996), ovoids were formed at the early stages of crystallization of the massif. The low content of Ta and Nb in them cannot be explained by the formation of columbite. Most likely this reflects the initial low concentration of these elements in the melt or is a consequence of crystallization of ilmenite, in which there are significant admixtures of Ta and Nb (up to 0.5–0.6 wt %).

Micas in the studied rocks are represented by the siderophyllite–Li-siderophyllite–zinnwaldite series (Fig. 5). Such an evolutionary trend in the mica composition is typical of A-type granite (Breiter et al., 2017). With an increasing degree of crystallization differentiation of rocks, the contents of F, Li, and other lithophile elements regularly increases in micas. This indicates the evolution of the residual melt composi-

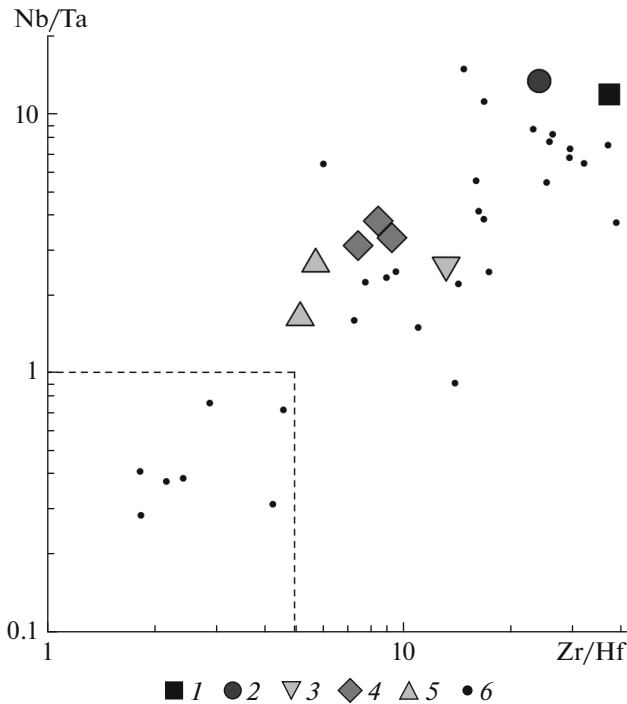


Fig. 3. The ratio of Nb/Ta in the rock to the indicator of the ore potential Zr/Hf, after (Zaraisky et al., 2008). (1) *Bt–Amp* granite; (2) *Bt* granite; (3) massive Li–F granite, Sample 403–13 (Larin, 2011); (4) Li–*Sdph* granite; (5) Li–F granite; (6) rocks of eastern Transbaikalia genetically related to the Orlovskoe, Etykinskoe, and Achikanskoe Ta–Nb deposits. The dashed line shows the promising ore-bearing Ta–Nb objects, after (Zaraisky et al., 2008).

tion in the magmatic chamber. Accumulation of these elements may cause significant changes in the phase relations in the system, such as a shift in the eutectic composition of the melt (Manning, 1981) and an increase in the solubility of hydrous fluid in the melt (Alferyeva et al., 2018b; Holz et al., 1993).

The concentration of volatile components (F and Cl) in rock does not provide a quantitative estimate of their concentration in the system during crystallization. Important sources of data on crystallization conditions include micas, which, due to the OH–Cl–F exchange, record the features of the fluid regime and the composition of volatile components in the system.

According to the data of X-ray spectral microanalysis, the concentrations of F in micas of Li–*Sdph* and Li–F granites are 2.5–3.2 and 5.4–6.4 wt %, while the F/Cl ratios are 12–28 and 423–1874, respectively. The contents of F in micas of biotite–hornblende ovoid granite and biotite granite are 0.9 and 1.4 wt %; F/Cl = 1.6–3 (Table 4). This indicates an increasing role of F and decreasing role of Cl in fluid with a decreasing degree of differentiation of the studied rocks.

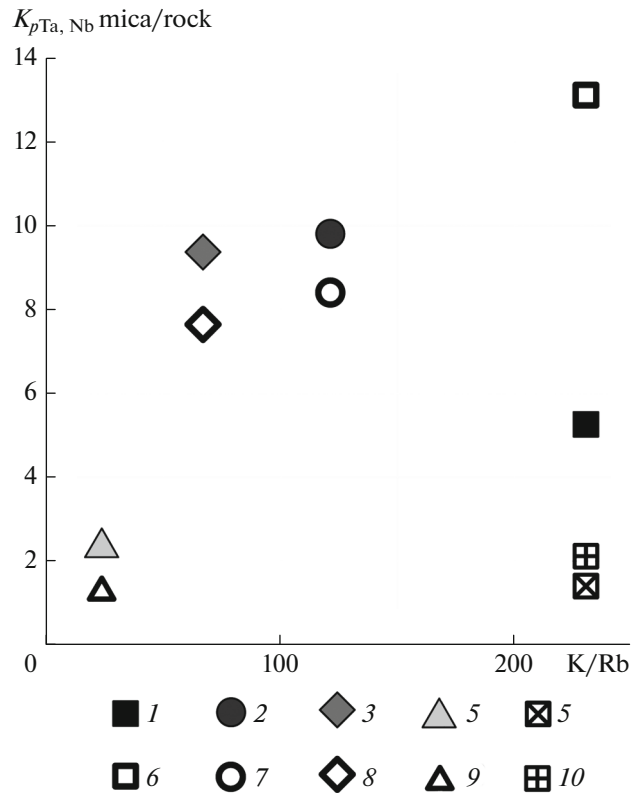


Fig. 4. The ratio of the concentration of Ta and Nb (ppm) in micas to their concentration in the rock vs. K/Rb ratio indicating crystallization differentiation of rocks, after (Aleksandrov, 1980). (1–5) K_{pTa} ; (6–10) K_{pNb} . (1 and 6) *Bt–Amp* granite; (2 and 7) *Bt* granite; (3 and 8) Li–*Sdph* granite; (4 and 9) Li–F granite; (5 and 10) *Bt–Amp* granite, for mica from potassium feldspar ovoids.

The semi-quantitative estimates of the F content in the natural magmatic fluid based on the mica composition, were performed using mineral geo-fluorimeters (Aksyuk, 2002). The concentration of HF (M, mol/dm³) in the natural fluid during the formation of mica was estimated as 0.02 M for ovoid biotite granite; 0.047 M, for biotite equigranular granite; and 0.24–0.34 M, for Li–F granite (Konyshev et al., 2017). It was assumed in the calculations that the activity of water is 1 and that Li replaces Mg isomorphically. In addition, it was necessary to know the temperature of the mica formation for the calculations. Such estimates of the formation are currently unavailable for Li–*Sdph* granite; thus, the content of F in the fluid was not estimated for this rock.

The trend of granite melt differentiation for the Salmi batholith is not unique. The formation of deeply differentiated granite varieties with the Ta–Nb mineralization at the final stages of crystallization was noted for the massifs of rapakivi granite, as well as for common biotite granite and syenite in different regions (Beskin, 2014). However, such estimates of the F content in the natural magmatic fluid are currently limited

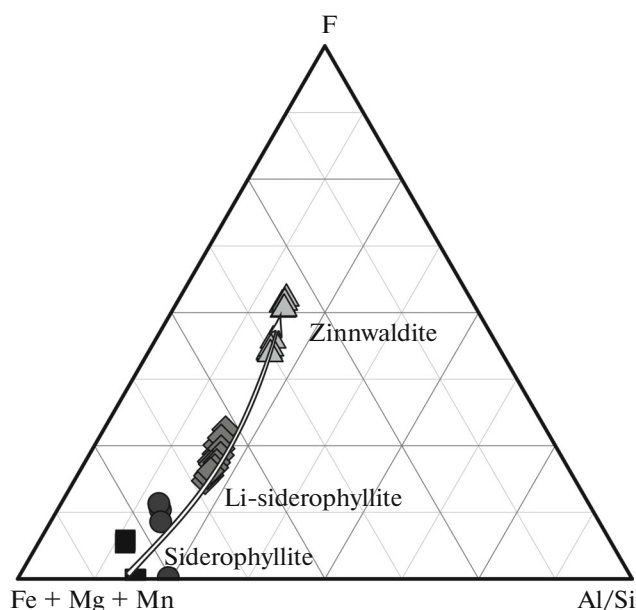


Fig. 5. A triangular diagram of the express classification of micas on the basis of the microprobe analysis. The arrow shows the trend of compositional variations in micas with increasing degree of crystallization differentiation of rocks. Individual analyses of micas are shown without averaging of the composition. The symbols on the diagram correspond to the rocks in Fig. 3.

for similar objects. As was shown by Aksyuk (2009), the fluid of the late-magmatic stage of consolidation of the Orlovskoe and Etykinskoe Ta–Nb deposits in eastern Transbaikalia contained 0.43 and 0.73 M HF, respectively. Rare-metal granite of these deposits was formed as the most differentiated variety of the biotite granite–Li–F amazonite granite series (Zaraisky, 2009; Syritso, 2001; Badanina, 2010). Comparison of the concentrations of HF in their fluids show that the conditions of the formation of the most differentiated granite varieties of the Salmi batholith are close to the conditions of the formation of the ore objects of eastern Transbaikalia.

CONCLUSIONS

Micas are indicators of the Ta–Nb mineralization existence in the studied granite series. A sharp decrease in the concentration of Ta and Nb in mica in relation to the content in the rock with an increase in the degree of crystallization differentiation and a high concentration of HF in the natural fluid is an indicator of favorable conditions for the formation of columbite.

ACKNOWLEDGMENTS

We are grateful to V.O. Yapaskurt, E.A. Minervina, A.I. Yakushev, N.V. Vasilyev, A.N. Nekrasov, D.A. Varlamov, and S.G. Simakin for active help in obtaining of the analyt-

ical data. Some analytical data were obtained at the Laboratory of Local Methods of Matter Study, Chair of Petrology, Department of Geology, Moscow State University, on a JEOL JXA-8230 electron microprobe, purchased by the Moscow University Development Program.

FUNDING

This study was supported by the Russian Foundation for Basic Research (project nos. 18-05-01101a and 14-05-31098 mol_a).

REFERENCES

- Aksyuk, A.M., Experimentally established geofluorimeters and the fluorine regime in granite-related fluids, *Petrology*, 2002, vol. 10, no. 6, pp. 557–569.
- Aksyuk, A.M., The fluorine regime in deep hydrothermal fluids and surface waters (experimental studies), *Extended Abstract of Doctoral (Geol.-Mineral.) Dissertation*, Moscow, Inst. Geokhim. Analit. Khimii Ross. Akad. Nauk, 2009.
- Acosta-Vigil, A., Buick, I., Hermann, J., Cesare, B., Rubatto, D., London, D., and Morgan, G.B., Mechanisms of crustal anatexis: A geochemical study of partially melted metapelitic enclaves and host dacite, SE Spain, *J. Petrol.*, 2010, vol. 51, pp. 785–821.
- Aleksandrov, I.V., *Geokhimiya rasseyannykh i rudnykh elementov v granitoidakh* (Geochemistry of Trace and Ore Elements in Granitoids), Nauka, Moscow, 1980.
- Alferyeva, Ya.O., Gramenitskiy, E.N., and Shchekina, T.I., Growth of Ta/Nb relation in residual granite melts (calculations based on experimental data from various sources), in *Tez. dokl. Vseross. ezhegodn. Sem. po eksperimental'noi mineralogii, petrologii i geokhimii, Ser. VESEMPG–2018, 18–19 aprelya 2018 g.* (Proc. Russ. Annu. Sem. Experiment. Miner., Petrol., Geochem. (RASEMPG–2018), April 18–19, 2018), Moscow, Inst. Geokhim. Analit. Khimii Ross. Akad. Nauk, 2018, pp. 140–142.
- Amelin, Yu.V., Larin, A.M., and Tucker, R.D., Chronology of multiphase emplacement of the Salmi rapakivi granite-anorthosite complex, Baltic Shield: implications for magmatic evolution, *Contrib. Mineral. Petrol.*, 1997, vol. 127, pp. 353–368.
- Anders, E. and Grevesse, N., Abundances of the elements: meteoritic and solar, *Geochim. Cosmochim. Acta*, 1989, vol. 53, pp. 197–214.
- Badanina, E.V., Syritso, L.F., Volkova, E.V., Thomas, R., and Trumbull, R.B., Composition of Li–F granite melt and its evolution during the formation of the ore-bearing Orlovka massif in Eastern Transbaikalia, *Petrology*, 2010, vol. 18, no. 2, pp. 131–157.
- Beskin, S.M., *Geologiya i indikatornaya geokhimiya tantal-niobievyykh mestorozhdenii Rossii (redkometal'nye granity)* (Geology and Indicator Geochemistry of Ta–Nb Deposits of Russia (Rare-Metal Granites)), Moscow: Nauchn. Mir, 2014.
- Breiter, K., Vaňková, M., Vašinová Galiová, M., Korbelová, Z., and Kanický, V., Lithium and trace-element concentrations in trioctahedral micas from granites of

- different geochemical types measured via laser ablation ICP–MS, *Min. Mag.*, 2017, vol. 81, no. 1, pp. 15–33.
- Gramenitskiy, E.N. and Shchekina, T.I., Behavior of rare earth elements and yttrium during the final differentiation stages of fluorine-bearing magmas, *Geochem. Int.*, 2005, vol. 43, no. 1, pp. 39–52.
- Irber W., The lanthanide tetrad effect and its correlation with K/Rb, Eu/Eu*, Sr/Eu, Y/Ho, and Zr/Hf of evolving peraluminous granite suites, *Geochim. Cosmochim. Acta*, 1999, vol 63, no. 3/4, pp. 489–508.
- Ivashchenko, V.I. and Golubev, A.I., New aspects of mineralogy and metallogeny of the Pitkäranta ore district, *Tr. KarNTs RAN*, 2015, no. 7, pp. 127–148.
- Konyshev, A.A., Anosova, M.O., and Minervina, E.A, Micas from granites of the Salmi pluton: varieties and indicator features, in *Mater. III mezhd. geol. Konf. "Granity i evolyutsiya Zemli: mantiya, kora i granitobrazovanie"* (Proc. III Int. Geol. Conf. "Granites and the Earth's Evolution: Mantle and Crust in the Granite Origin"), Yekaterinburg, 2010, pp. 133–135.
- Kovalenko, V.I., Koval', P.V., Konusova, V.V., Smirnova, E.V., and Balashov, Yu.A., Rare-earth geochemistry in intrusive rocks of the calc-alkali series, *Geochem. Int.*, 1983, vol. 20, no. 1, pp. 111–126.
- Larin, A.M., *Granity rapakivi i assotsiiruyushchie porody* (Rapakivi Granites and Associated Rocks), St. Petersburg, Nauka, 2011.
- Masuda, A., Kawakami, O., Dohmoto, Y., and Takenaka, T., Lanthanide tetrad effects in nature: Two mutually opposite types W and M, *Geochim. Cosmochim. Acta*, 1987, no. 22, pp. 119–124.
- Nash, W. and Crecraft, H., Partition coefficients for trace elements in silicic magmas:, *Geochim. Cosmochim. Acta*, 1985, vol. 49, pp. 2309–2322.
- Neymark, L.A., Amelin, Yu.V., and Larin, A.M., Pb Nd Sr isotopic and geochemical constraints on origin of the 1.54–1.56 Ga Salmi rapakivi granite–anorthosite batholith (Karelia, Russia), *Mineral. Petrol.*, 1994, vol. 50, pp. 173–193.
- Pavlov, G.M., The layering in near-surface rare-metal Li–F granite pluton of in north Ladoga region, *Phd Thesis*, Moscow: Mosk. Gos. Univ, 1991. (in Russian).
- Peretyazhko, I.S. and Savina, E.A., Tetrad effects in the rare earth element patterns of granitoid rocks as an indicator of fluoride-silicate liquid immiscibility in magmatic systems, *Petrology*, 2010, vol. 18, no. 5, pp. 514–543.
- Shebanov, A.D., Belyaev, A.M., and Savatenkov, V.M., The significance of residual source material (restite) in rapakivi granite petrogenesis: an example from Salmi batholith, Russian Karelia, in *Symp. on Rapakivi Granites and Related Rocks. Abstract Vol.*, Haapala, I., Ramo, O.T., and Kosunen, P., Eds., Helsinki, Finland: Helsinki. Univ. Press, 1996.
- Syritso, L.F., Tabuns, E.V., Volkova, E.V., Badanina, E.V., and Vysotskii, Yu.A., Geochemical model of the genesis of Li–F granites in the Orlovka Massif, Eastern Transbaikalia, *Petrology*, 2001, vol. 9, no. 3, pp. 313–336.
- Tischendorf, G., Gottesmann, B., Förster, H.J., and Trumbull, R.B., On Li-bearing micas: estimating Li from electron microprobe analyses and an improved diagram for graphical representation, *Min. Mag.*, 1997, vol. 61, no. 6, pp. 809–834.
- Vasilyev, N.V. and Borodulin, G.P., About Nb and Ta in lithium micas, in *Mater. mezhd. konf. "Geokhimiya magmaticheskikh porod". Shkola "Shchelochnoi magmatizm Zemli", g. Koktebel'* (Proc. Int. Conf. "Geochemistry of Magmatic Rocks". School "Alkaline Magmatism of the Earth", Koktebel), 2010.
- Veksler, V.I., Dorfman, A.M., Kamenetsky, M., Dulski, P., and Dingwell, D.B., Partitioning of lanthanides and Y between immiscible silicate and fluoride melts, fluorite and cryolite and the origin of the lanthanide tetrad effect in igneous rocks, *Geochim. Cosmochim. Acta*, 2005, vol. 69, no. 11, pp. 2847–2860.
- Yasnygina, T.A. and Rasskazov, S.V., Tetrad effect in rare earth element distribution patterns: Evidence from the Paleozoic granitoids of the Oka zone, eastern Sayan, *Geochem. Int.*, 2008, vol. 46, no. 8, pp. 814–825.
- Zaraisky, G.P., Aksyuk, A.M., Devyatova, V.N., Udoratina, O.V., and Chevychelov, V.Yu., Zr/Hf ratio as an indicator of fractionation of rare-metal granites by the example of the Kukulbei complex, Eastern Transbaikalia, *Petrology*, 2008, vol. 16, no. 7, pp. 710–736.
- Zaraisky, G.P., Aksyuk, A.M., Devyatova, V.N., Udoratina, O.V., and Chevychelov, V.Yu., The Zr/Hf ratio as a fractionation indicator of rare-metal granites, *Petrology*, 2009, vol. 17, no. 1, pp. 25–45.

Translated by A. Bobrov